

Impact of Particle Size on Room Temperature Ferrimagnetism of SrFe₁₂O₁₉

Neeraj Kumar · Anuj Kumar · R. Jha · Anjana Dogra ·
Renu Pasricha · R.K. Kotnala · Hari Kishan ·
V.P.S. Awana

Received: 28 October 2009 / Accepted: 16 February 2010 / Published online: 3 March 2010
© Springer Science+Business Media, LLC 2010

Abstract In this paper, we report the control of important hysteresis parameters, which are useful for memory devices, viz. M_s , H_c and M_r/M_s , by changing the particle size/calcination temperature. An investigation of SrFe₁₂O₁₉ nanopowder from the structural and magnetic aspect is performed using X-ray diffraction (XRD), High Resolution Transmission Electron Microscopy (HRTEM), Scanning Electron Microscopy (SEM) and Vibrating Sample Magnetometer (VSM). The average particle size (APS) of SrFe₁₂O₁₉(nanopowder) increases from 26 to 600 nm with calcination temperatures of 400 and 1100 °C in air, respectively. With the increase in calcination temperature, saturation magnetization (M_s) increases with the decrease in coercivity for the respective sample. The change in saturation magnetization and coercive field are explained on the basis of transition from single domain structure to multi-domain geometry with an increase in the heating temperature. The sample heated at 1000 °C shows a minimum coercive field (2.71 kOe) and an appropriate squareness ratio (M_r/M_s) compared to other calcined samples.

Keywords Ferrites · X-ray diffraction · Magnetization

1 Introduction

M-type magnetic hard ferrites such as SrFe₁₂O₁₉ and BaFe₁₂O₁₉ are known to be interesting ferrimagnetic ox-

ides. Their attractive magnetic properties such as high intrinsic coercivity originated from high magneto-crystalline anisotropy make them potential candidates for variety of applications. In fact, due to a combination of good magnetic properties, chemical stability and low cost, barium and strontium hexaferrite are widely used as permanent magnet materials as well as in magnetic recording media [1, 2]. Interestingly, in the case of hexaferrites the crystallites are even expected in single domain state and high magnetic coercivity strongly depends on crystalline anisotropy within easy magnetization axis. The M-type hexagonal SrFe₁₂O₁₉ crystallize with 64 ions per unit cell on 11 different symmetry sites [3]. In the magnetic structure given by Gorter model, 24 Fe³⁺ atoms are arranged over five distinct sites: three octahedral sites and two tetrahedral sites. These five sites are coupled via ferromagnetic super-exchange interaction through O²⁻ ions. It is very well known from the literature that the magnetic properties like saturation magnetization, coercivity, etc., of the hexaferrites depend on particle (crystallite) size and shape [4–7]. Therefore, apart from bulk hexaferrites the nanoparticles of the hexaferrites also received much attention from the researchers. Nanoparticles of the material exhibit significantly different properties from their bulk counterpart. Vijayalakshmi et al. [8] reported the synthesis of nano-SrFe₁₂O₁₉ particles with citrate precursor method in different Fe/Sr mole ratio. They observed ferrimagnetic along with superparamagnetic nature and explained the formation of single domain enhanced by Sr ions. Recently, Wang reported a correlation between magnetic properties and particles morphology, i.e. needle-like, rod-like, bubble nano-SrFe₁₂O₁₉ and spherical nano-SrFe₁₂O₁₉ [9]. The needle-like SrFe₁₂O₁₉ particles have the maximum coercivity among all. By controlling the microstructure, morphology and chemical composition and particle size, the magnetic

N. Kumar · A. Kumar · R. Jha · A. Dogra · R. Pasricha ·
R.K. Kotnala · H. Kishan · V.P.S. Awana (✉)
National Physical Laboratory, Dr. K.S. Krishnan Marg (CSIR),
New Delhi 110012, India
e-mail: awana@mail.nplindia.ernet.in
url: www.freewebs.com/vpsawana/

properties of the material can be improved. Such different size particles can be produced by various synthesis techniques as chemical co-precipitation method [10], high-energy ball mill method [11], sol-gel [12], glass crystallization [13], citrate precursor [14], and salt melt methods [15], and also their physical properties can be controlled.

From the above discussion, one concludes that the magnetic properties of hexaferrites strongly depend on the size and shape of the particles. Therefore, in our present study we focus on the effect of heating treatments at various temperatures on the microstructural and magnetic behavior of the nano strontium hexaferrite ($\text{SrFe}_{12}\text{O}_{19}$).

2 Experimental

The standard nanopowder of $\text{SrFe}_{12}\text{O}_{19}$ was purchased from Sigma Aldrich and used as initial raw material. As the properties of this magnetic material strongly depend on the purity of the powder, we used highly pure raw powder of 99.99% purity. This corroborated powder was then heated at various temperatures, viz. 400, 800, 1000, and 1100 °C in air each for 6 hrs, then cooled by 2 °C/min to room temperature. The X-ray diffraction (XRD) patterns of all samples were recorded using Rigaku machine with Cu-K_α ($\lambda = 1.54 \text{ \AA}$) radiation. For the structural morphology, high-resolution transmission electron microscopy (HRTEM), JEOL, JEM 200CX instrument was used. Scanning electron microscopy (SEM, TESCAN VEGA make) studies were also performed. Magnetization measurements at room temperature were carried out on Lakeshore Vibrating Sample Magnetometer (VSM).

3 Results and Discussion

Standard nano- $\text{SrFe}_{12}\text{O}_{19}$ powder (average particle size around 20–40 nm) was used as the initial material. Figure 1 depicts the room temperature XRD patterns of all samples heated at various temperatures: 400, 800, 1000, and 1100 °C in air. In comparison to observed values of analogous peaks corresponding to the crystal structure and the JCPDS card (24-1207), it can be concluded that all the samples crystallize in single $\text{SrFe}_{12}\text{O}_{19}$ phase without any trace of impurity peaks. As an illustration, from the patterns of initial and heated samples, the X-ray line broadening decreased with increasing the heating temperature. The sharpening of peaks with the increase in heating treatment temperature can be correlated to the increase in the average particle size.

In order to visualize the average particle size in detail, the high-resolution transmission electron microscopy

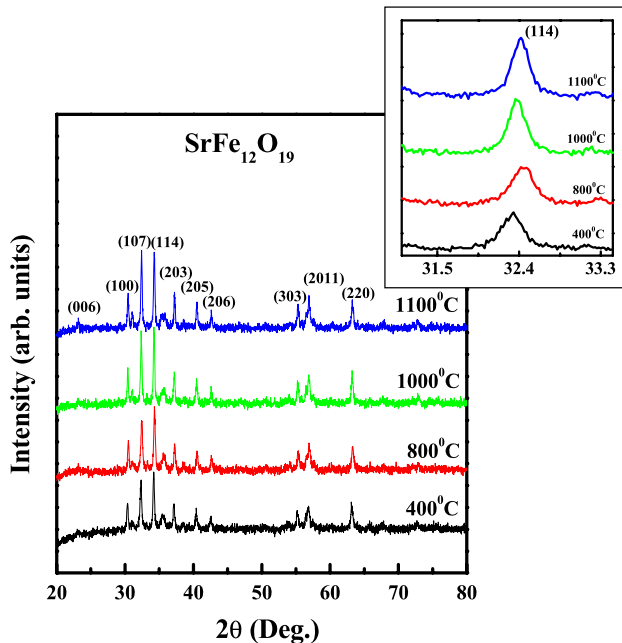


Fig. 1 X-ray diffraction patterns of nano- $\text{SrFe}_{12}\text{O}_{19}$ heated at various temperatures in air

(HRTEM) was performed. Images depicted from HRTEM for the powders heated at 400 and 1100 °C are shown in Fig. 2(a) and (b). TEM photograph shows that the sample heated at 400 °C is in a well-dispersed spherical shape. From the images we observe an increase in particle size with an increase in the heating treatment temperature, as expected. With the increase in temperature large particles are formed at the expense of small particles due to the increase in the diffusion rate. Further, in support of our TEM micrographs/particle size, we carried out SEM measurements. Figure 3(a–d) shows the SEM images for the pristine powder and the powders heated at 800, 1000 and 1100 °C. From the SEM images, we clearly observe an increase in average particle size from 26 nm (pristine) to 600 nm (1100 °C) with the increase in the sintering temperature.

Magnetization hysteresis, $M(H)$, curves for the powders of $\text{SrFe}_{12}\text{O}_{19}$ heated at different temperatures are shown in Fig. 4. The saturation magnetization (M_s) and coercive field (H_c) extracted from the $M(H)$ loop are shown in Table 1. From Fig. 4, it is observed that the coercive field decreases (except for the 1100 °C heated samples) with the increase in the sintering temperature. This result can be explained on the basis of the obtained transformation of the single domain to multi-domain structure, when the particle size increases after sintering. In the case of the single domain, magnetization is due to the rotation of magnetization which leads to a large coercive field, whereas in the case of the multi-domain structure magnetization takes place through the displacement of

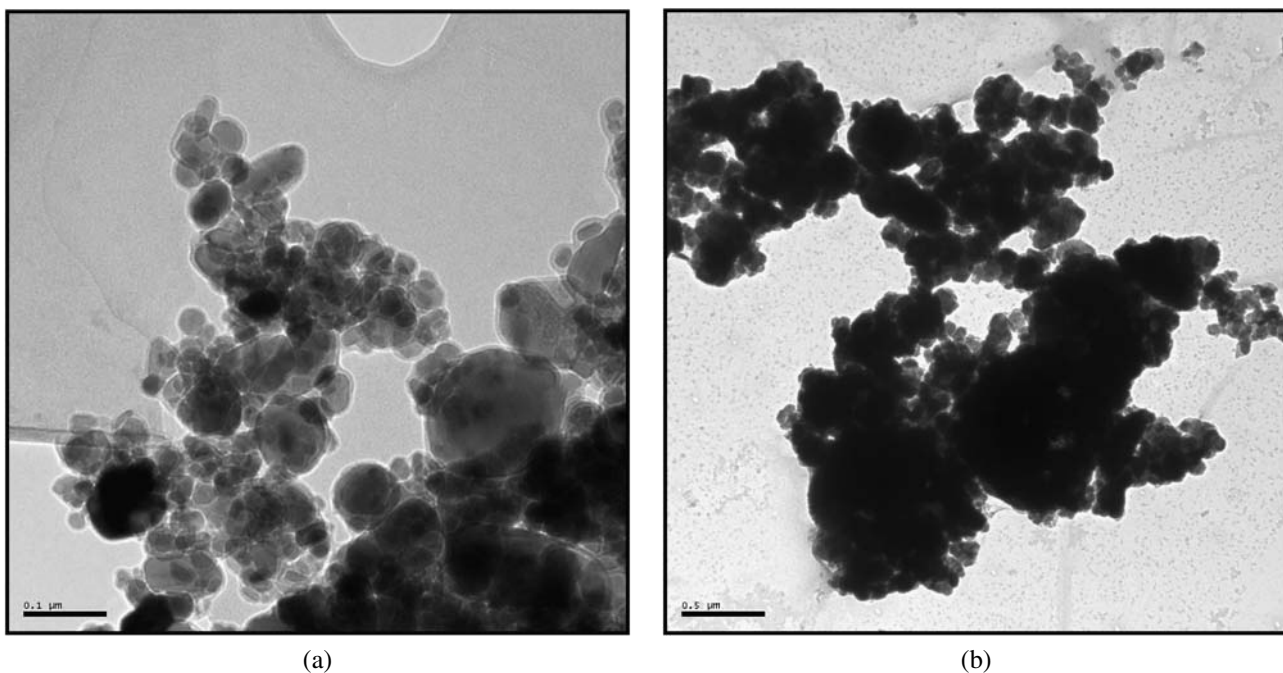


Fig. 2 (a) HRTEM micrograph of $\text{SrFe}_{12}\text{O}_{19}$ heated at $400\text{ }^\circ\text{C}$. Size $\sim 20\text{--}60\text{ nm}$. (b) HRTEM micrograph of $\text{SrFe}_{12}\text{O}_{19}$ heated at $1100\text{ }^\circ\text{C}$

the domain wall which leads to a small coercive field [16]. For the single domain structure, the average particle size is given as [17]:

$$D_{m(\text{crit})} = 9\sigma_w / 2\pi M_s^2,$$

where σ_w is the domain wall density energy depending on magneto-crystalline anisotropy, Curie temperature; and M_s is the saturation magnetization. Zi et al. [18] explained the relation between single domain and multi-domain in $\text{SrFe}_{12}\text{O}_{19}$ on the basis of $D_{m(\text{crit})}$. They assumed $D_{m(\text{crit})}$ for $\text{SrFe}_{12}\text{O}_{19}$ to be about 650 nm. Also Otani et al. [19] proposed that the grain size for the single domain should not exceed the critical size, $D_{m(\text{crit})}$. Along the same lines, Rezlescu et al. [20] observed an increase in coercivity (H_c) with an increase in domain size and suggested a mono-domain behavior of the grains. As the particle size increases from 26 nm for the pristine sample to ~ 600 nm for $1100\text{ }^\circ\text{C}$ heated samples, we approach the multi-domain structure; hence, there is a decrease in the coercive field (H_c). The sample heated at $1000\text{ }^\circ\text{C}$ has minimum coercivity of 2.719 kOe. A further increase in calcination temperature decreases this magnetic parameter. This abrupt behavior may be either particle size/shape effect or may be associated with crystal anisotropy [18]. Magnetic properties in these materials, such as orientation of magnetic domains and microstructure, matter very much.

We observe that the saturation magnetization gradually increases for the powders heated at higher temperatures ex-

cept for the $1100\text{ }^\circ\text{C}$ heated samples. The saturation magnetization can also be explained on the basis of domain structure. The increase in M_s might be due to the increase in particle size since it is known that the energy of the magnetic particle in an external field is proportional to the particle size [21]. Moreover, the spin canting phenomenon is also reduced with an increase in the particle size at higher temperature calcinations. The observed values of saturation magnetization and coercivity for the sample calcinated at $1000\text{ }^\circ\text{C}$ are very close to the theoretical M_s value of 74.3 emu/g of the single crystal strontium ferrite [2, 4]. Low coercive field and high saturation magnetization strontium ferrites are very suitable for magnetic recording applications [1, 2]. Also the squareness ratio, M_r/M_s , which gives the squareness of the hysteresis loop, is about 0.50 for the sample heated at $1000\text{ }^\circ\text{C}$ along with an appropriate low value of the coercive field. The inset of Fig. 4 shows the variation of saturation magnetization and coercivity with calcination temperature. This result clearly indicates that with an increase in the sintering temperature, we are moving from the single domain to multi-domain geometry since the field required for saturating the multi-domain specimen is larger than the field required for saturating the single domain. Thus we can say that the samples heated at higher temperatures are much softer magnetic materials compared to the powders heated at lower temperatures or the pristine powder.

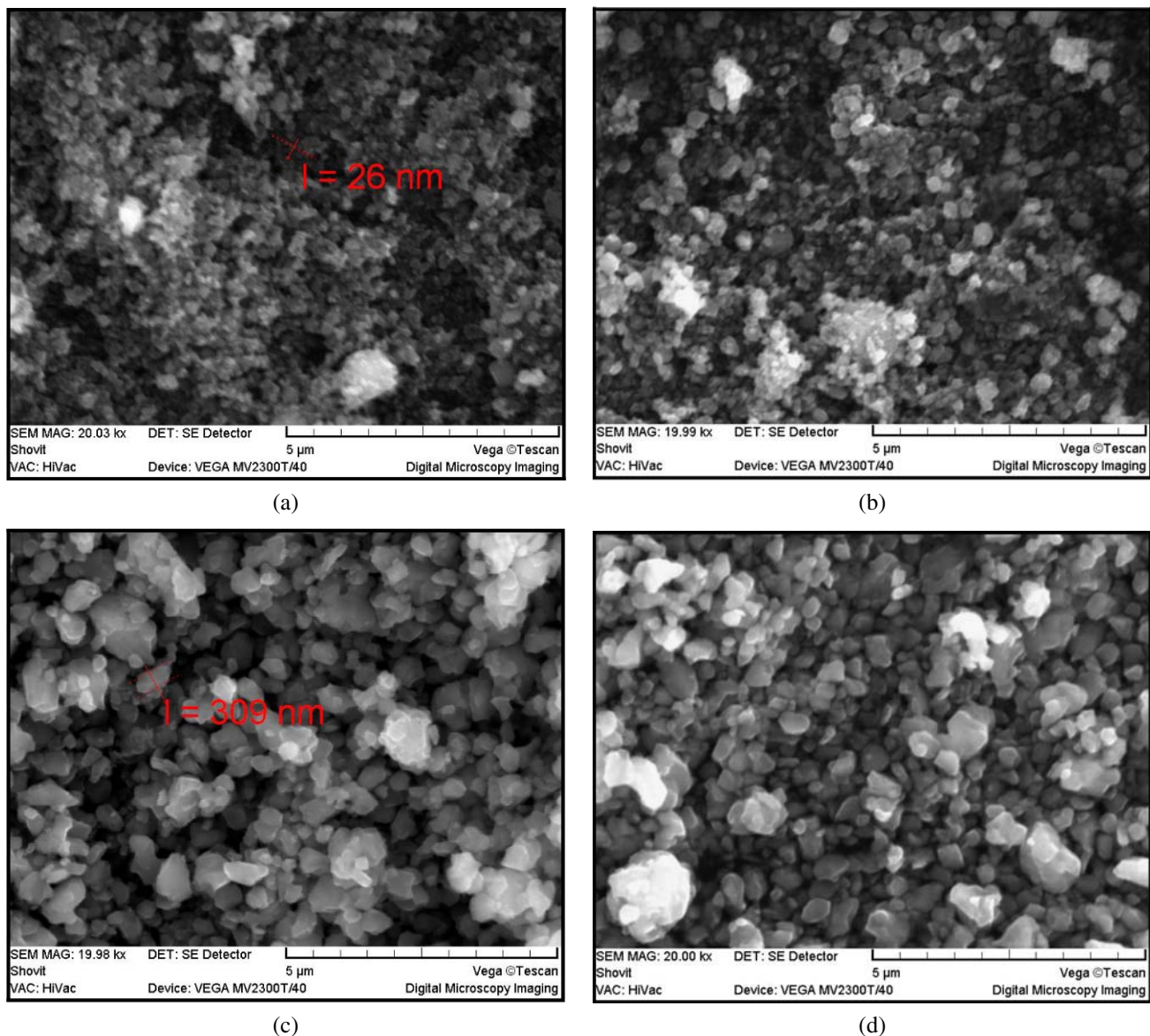


Fig. 3 (a) SEM image of pristine $\text{SrFe}_{12}\text{O}_{19}$. (b) SEM image of $\text{SrFe}_{12}\text{O}_{19}$ heated at $800\text{ }^{\circ}\text{C}$. (c) SEM image of $\text{SrFe}_{12}\text{O}_{19}$ heated at $1000\text{ }^{\circ}\text{C}$. (d) SEM image of $\text{SrFe}_{12}\text{O}_{19}$ heated at $1100\text{ }^{\circ}\text{C}$

Table 1 Values of saturation magnetization (M_s), squareness ratio (M_r/M_s) and coercivity (H_c) of the sample $\text{SrFe}_{12}\text{O}_{19}$ heated at different temperatures

Sample	M_s (emu/g)	M_r/M_s	H_c (kOe)
400 °C	54.930 ± 1.1	0.5544	4.5870 ± 0.09
800 °C	64.591 ± 1.3	0.5372	4.3540 ± 0.08
1000 °C	82.958 ± 1.7	0.5028	2.7190 ± 0.05
1100 °C	50.835 ± 1.0	0.5447	4.3090 ± 0.08

4 Conclusion

Standard nano- $\text{SrFe}_{12}\text{O}_{19}$ samples were subjected to different heat treatments. From the analysis of various character-

ization techniques like XRD, HRTEM, SEM, and magnetization, we observe that the structure remained intact at different heating temperatures. We observed an increase in the particle size from 26 to ~ 600 nm with an increase in the heating temperature for pristine and $1100\text{ }^{\circ}\text{C}$ heated sample. As for the magnetization parameters, the M_r/M_s ratio decreased, which indicates an increase in squareness of the hysteresis loop. The sample heated at $1000\text{ }^{\circ}\text{C}$ had minimum coercivity (2.719 kOe) and maximum saturation magnetization (82.958 emu/g). The variations of H_c and M_s were explained on the basis of the evolution of multi-domain structure with the increase in the heating treatment temperature of the sample.

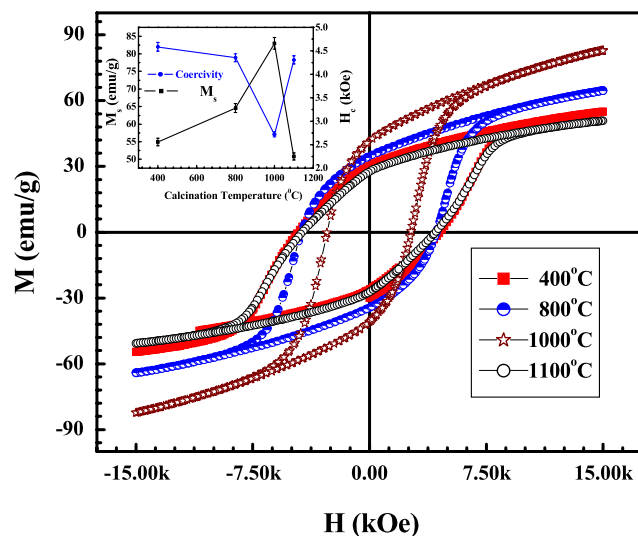


Fig. 4 M–H loop of SrFe₁₂O₁₉ heated at different temperatures

Acknowledgements The authors would like to thank Prof. Vikram Kumar, Director of the National Physical Laboratory, for his constant support and encouragement. One of the authors Neeraj Kumar also would like to thank CSIR for financial support through Diamond Jubilee Research Intern Award Scheme.

References

- Brassard, S., Champigny, B.: In: Dempsey, N.M., deRango, P. (eds.) Proceedings of 18th International Workshop on High Performance Magnets and Their Applications, Annecy, France, 29 August–2 September, vol. 1, p. 22 (2004)
- Karabasov, Yu.S. (ed.) New Materials. MISiS, Moscow (2002)
- Wang, J.F., Paonton, C.B., Harris, I.R.: *J. Magn. Magn. Mater.* **298**, 122 (2006)
- Ataei, A., Heshmati-Manesh, S.: *J. Eur. Ceram. Soc.* **21**, 1951 (2001)
- García-Cerda, L.A., Rodríguez-Fernández, O.S., Reséndiz-Hernández, P.J.: *J. Alloys Compd.* **369**, 182 (2004)
- Fu, Y.P., Lin, C.H., Pan, K.Y.: *J. Alloys Compd.* **349**, 228 (2003)
- Ding, J., Miao, W.F., McCormick, P.G., Street, R.: *J. Alloys Compd.* **281**, 32 (1998)
- Vijayalakshmi, A., Gajbhiye, N.S.: *J. Appl. Phys.* **83**, 400 (1997)
- Wang, Y., Li, Q., Zhang, C., Li, B.: *J. Alloys Compd.* **467**, 284 (2009)
- Liu, X., Wang, J., Gan, L.M., Ng, S.C.: *J. Magn. Magn. Mater.* **195**, 452 (1999)
- Ketov, S.V., Yagodkin, Yu.D., Lebed, A.L., Chernopyatova, Yu.V., Khlopkov, K.: *J. Magn. Magn. Mater.* **300**, e479 (2006)
- Tenaud, P., Morel, A., Kools, F., Breton, J.M., Lechevallier, L.: *J. Alloys Compd.* **370**, 331 (2004)
- Liu, X., Wang, J., Gan, L.M., Ng, S.C.: *J. Magn. Magn. Mater.* **184**, 344 (1998)
- Topal, U., Ozkanb, H., Dorosinskii, L.: *J. Alloys Compd.* **428**, 17 (2007)
- Bernier, J.C.: *Mater. Sci. Eng.* **233**, 109A (1989)
- Cullity, B.D.: Introduction to Magnetic Material. Addison-Wesley, Reading (1972)
- Smith, J., Wijn, H.P.J.: Les Ferrites. Dunod, Paris (1961)
- Zi, Z.F., Sun, Y.P., Zhu, X.B., Yang, Z.R., Dai, J.M., Song, W.H.: *J. Magn. Magn. Mater.* **320**, 2746 (2008)
- Otani, Y.: In: Hadjipapay, G.C., Prinz, G.A. (eds.) Science and Technology of Nanostructured Magnetic Materials, p. 695. Plenum, New York (1991)
- Rezlescu, L., Rezlescu, E., Popa, P.D., Rezlescu, N.J.: *J. Magn. Magn. Mater.* **193**, 288 (1999)
- Chen, D.-H., Chen, Y.-Y.: *Mater. Res. Bull.* **37**, 801 (2002)